

Brief Reports:**Non-invasive monitoring of glycemia-induced regulation of GLP-1R
expression in murine and human islets of langerhans**

Running title: Non-invasive monitoring of GLP-1R regulation

**Mijke Buitinga^{1,2*}, Christian M.Cohrs^{3,4,5}, Wael A.Eter¹, Lieke Claessens-Joosten¹,
Cathelijne Frielink¹, Desirée Bos¹, Gerwin Sandker¹, Maarten Brom¹, Stephan
Speier^{3,4,5}, Martin Gotthardt¹**

Word count: 2083

Figure count: 4

Author affiliations:

¹Department of Radiology and Nuclear Medicine, Radboudumc, Nijmegen, The Netherlands

²Department of Clinical and Experimental Endocrinology, KU Leuven, Leuven, Belgium

*³Paul Langerhans Institute Dresden of Helmholtz Zentrum München at the University Clinic Carl Gustav
Carus of Technische Universität Dresden, Helmholtz Zentrum München, 85764 München-Neuherberg,
Germany*

⁴German Center for Diabetes Research, 85764 München-Neuherberg, Germany

⁵Institute of Physiology, Faculty of Medicine, Technische Universität Dresden, Germany

***Corresponding author:**

Dr. M.Buitinga

Clinical and Experimental Endocrinology, KU Leuven

O&N I Herestraat 49 - bus 902

3000 Leuven, Belgium

E-mail: mijkebuitinga@hotmail.com

Tel: +31 6 81 35 68 01

Tweet: M.Buitinga et al., led by prof. M Gotthardt and prof. S.Speier used non-invasive imaging techniques to demonstrate a hyperglycemia-induced reduction of GLP-1R mediated exendin uptake in murine and human islets that could be restored upon normalization of blood glucose levels. #GLP-1R imaging #non-invasive imaging techniques #GLP1 receptor regulation.

Abstract

GLP-1R imaging with radiolabelled exendin has proven to be a powerful tool to quantify beta-cell mass (BCM) *in vivo*. As GLP-1R expression is thought to be influenced by glycemic control, we examined the effect of blood glucose levels on GLP-1R-mediated exendin uptake in both murine and human islets and its implications for BCM quantification. Periods of hyperglycemia significantly reduced exendin uptake in murine and human islets, which was paralleled by a reduction in GLP-1R expression. Detailed mapping of the tracer uptake and insulin and GLP-1R expression conclusively demonstrated that the observed reduction in tracer uptake directly correlates to GLP-1R expression levels. Importantly, the linear correlation between tracer uptake and beta-cell area was maintained in spite of the reduced GLP-1R expression levels. Subsequent normalization of blood glucose levels restored absolute tracer uptake and GLP-1R expression in beta-cells and the observed loss in islet volume was halted.

This manuscript emphasizes the potency of nuclear imaging techniques to monitor receptor regulation non-invasively. Our findings have significant implications for clinical practice, indicating that blood glucose levels should be near-normalized for at least three weeks prior to GLP-1R agonist treatment or quantitative radiolabeled exendin imaging for BCM analysis.

Introduction

As a decline in functional beta-cell mass (BCM) contributes to diabetes development, current drug development is geared towards compounds that can prevent beta-cell death or increase BCM (1). Autopsy studies in patients with both type 1 (2,3) and type 2 (4) diabetes have demonstrated residual BCM, even decades after disease onset, supporting the notion that beta-cell enhancing strategies can be promising in humans suffering from diabetes. While numerous studies report on bioactive molecules that can induce beta-cell proliferation or protection in animals (1,5), translation of these compounds to humans is hampered by the inability to measure BCM. As biopsying the human pancreas is associated with an unacceptable complication rate (6), a biomarker that reliably reflects BCM would be imperative to demonstrate the efficacy of candidate compounds in humans (7). Furthermore, such a biomarker would aid decision making early in the drug development process, and allow for patient stratification to identify patients with residual BCM who would be eligible for therapy.

We have previously developed a non-invasive imaging technology to quantify BCM based on the radiolabeled GLP-1 analog exendin (8). Preclinical studies demonstrated that pancreatic uptake of exendin linearly correlates with BCM (9) and that both off-target specific and non-specific binding are negligible in non-human primate pancreata (10). The first clinical study revealed marked differences in pancreatic uptake between patients with type 1 diabetes and controls (8). In line with the autopsy studies (2,3), residual exendin uptake was found in two out of five patients, illustrating the potential of this imaging

strategy which is currently considered the most advanced approach to non-invasively quantify BCM (7).

Nevertheless, there are indications that hyperglycemia down-regulates GLP-1R expression (11,12) and signaling (12) in beta-cells *in vitro*, possibly affecting GLP-1R based BCM quantification in diabetic individuals. Here, we examined the effect of chronic hyperglycemia and subsequent normalization of blood glucose levels on GLP-1R mediated exendin uptake in both murine and human islets and its implications for BCM quantification. For this, we used an islet transplantation setup in a chemically-induced diabetic mouse model as this allows control over islet-cell mass and glycemic stress exposure.

Research Design and Methods

Animal Models and Human Islets

Animal experiments were approved by the Animal Welfare Committee of the Radboud University (The Netherlands) or the German Center for Diabetes Research (Germany) and carried out in accordance with the local and national guidelines. Female C3H/HeNCrl (Charles River, Italy) and male NOD.CB17-*Prkdc*^{scid}/J (NOD-Scid) mice (Jackson Laboratories, USA) were used for syngeneic and allogeneic islet transplantations, respectively. Human islets were obtained from a 37 year-old non-diabetic female organ donor (BMI 19.57 kg/m², HbA1c 4.6%, 90% viability and purity; tebu-bio, France).

Radiolabeling

Mice were injected with 0.1 µg ¹¹¹In labeled [Lys40(DTPA)]exendin-3 (Peptide Specialty Laboratories, Germany) (±15 MBq), as previously described (13).

Syngeneic Islet Transplantation and Imaging

For the induction of hyperglycemia, C3H/HeNCrl mice were injected i.v. with 100 mg/kg Alloxan (Sigma, USA). Blood glucose levels were measured three times a week. After hyperglycemia was confirmed, mice received subcutaneous insulin implants (LinShin, Canada) to normalize blood glucose levels (14). Syngeneic islets were isolated from 8-10 week-old mice by collagenase digestion and 200 islets were transplanted in the calf muscle, as previously described (15). Two weeks after transplantation, mice were randomly assigned to one of three experimental groups. The blood glucose levels of the control group

were maintained <200 mg/dL. Insulin pellets were removed from mice assigned to the Hyper or Restored group to re-induce hyperglycemia (>350 mg/dL). After four weeks of hyperglycemia, the RESTORED group received insulin pellets again. At the end of the experiment, mice were injected with radiolabeled exendin-3 and scanned 1 hour after injection on a small animal U-SPECT-II/ CT system (MILabs, The Netherlands) with a 1 mm multi-pinhole ultra-high sensitivity mouse collimator for 50 minutes. Two hours after injection, mice were sacrificed and grafts were embedded in paraffin for histology and autoradiography.

Autoradiography

4- μ m-thick sections from different levels of the islet grafts were exposed to an imaging plate (Fuji Film BAS-SE 2025, Raytest, Germany) for one week. Images were visualized with a Typhoon FLA 7000 laser scanner (GE Healthcare Life Sciences). Tracer uptake quantification was done with AIDA Image Analyzer software (Raytest GmbH, Germany). To normalize the uptake to the insulin area, sections were stained for insulin (see Immunohistochemistry and morphometric analysis).

Human Islet Transplantation into the Eye, STZ Treatment and longitudinal in vivo Imaging

Eight-week-old male NOD.CB17-*Prkdc*^{scid}/J (NOD-Scid) mice were used as transplant recipients. Upon arrival, human islets were cultured overnight in CMRL-1066 (Corning cellgro; VA), supplemented with 2 g/L human serum albumin, 100 unit/mL

penicillin/streptomycin. Mice were transplanted with 15 islets into the anterior chamber of the eye as previously described (16). Islets were allowed to engraft for 8 weeks as human islets require a prolonged time for proper revascularization and engraftment. Hyperglycemia was induced by injecting 150 mg/kg streptozotocin (STZ) (Sigma-Aldrich, Germany) and blood glucose levels were monitored. To restore normoglycemia, insulin pellets were implanted after 7 weeks of hyperglycemia.

Four hours prior to imaging, mice were injected i.v. with 4nmol exendin3-Alexa647 in PBS. Mice were intubated and anesthetized by 2% isoflurane in 100% oxygen. To limit pupil dilation and iris movement, 0.4% pilocarpine (Pilomann; Bausch & Lomb, USA) was placed on the cornea. Repetitive *in vivo* imaging was performed at indicated time points on an upright laser scanning microscope (LSM780 NLO; Carl Zeiss, Germany) with a water dipping objective (W Plan-Apochromat 203/1.0 DIC M27 75 mm; Carl Zeiss) using vidisic eye gel (Bausch & Lomb, USA) as immersion. The total volume of transplanted islets was assessed by detecting 633 nm laser backscatter. Exendin3-Alexa647 uptake was assessed by spectral analysis on an internal array GaAsP detector at a resolution of 8.7 nm using the lambda unmixing algorithm of ZEN2009 (Zeiss, Germany), using combined, 488 nm, 561 nm and 633 nm laser excitation. Reference spectra were acquired for exendin3-Alexa647 after *in vivo* labeling and for human islet autofluorescence from transplanted human islets without labeling. Islet volume was determined by semiautomatic volume creation and exendin3-Alexa647 by automatic surface rendering from median filtered Z-stacks with Imaris 8.1 (Bitplane AG, Switzerland).

Immunohistochemistry and morphometric analysis

Paraffin sections of murine grafts were immunostained for insulin (17), or GLP1R. For the latter, pronase (1mg/mL, 10 min, 37 °C) was used as antigen retrieval. After blocking with 3% H₂O₂ (10min), sections were immunostained with mouse anti-GLP-1R (Novo Nordisk, Denmark, 1:50, o/n, 4 °C) followed by HRP-conjugated secondary antibody (DAKO, Copenhagen, Denmark, 1:100, 30 min). The staining was developed with DAB (Immunologic BV, The Netherlands) and sections were counterstained with hematoxylin. Morphometric analysis was performed with the trainable Weka segmentation plugin in ImageJ/Fiji (<http://rsb.info.nih.gov/ij/>).

Islet-containing eyes were fixed in PFA and mounted in TissueTek. 10µm-thick cryosections were prepared and immunostaining was performed with guinea-pig anti-insulin (1:200; Dako, Germany) and mouse anti-glucagon (1:2000; Sigma-Aldrich, Germany). Secondary antibodies goat anti-guinea-pig Alexa Fluor-488 and goat anti-mouse Alexa Fluor-633 (both 1:200; Thermo Fisher, Germany) were used and sections were counterstained with DAPI.

Statistical analysis

Statistical analysis was performed using SPSS version 22 (SPSS, USA). P-values less than 0.05 were considered statistically significant. Results were presented as mean±SEM. Group comparisons were performed using analysis of variance (ANOVA) with Tuckey post-hoc test or Mann-Whitney rank sum test, as indicated. Results obtained from longitudinal *in vivo* imaging studies were analyzed by linear mixed models (18).

Data and Resource Availability

The data sets generated and/or analyzed during the current study are available from the corresponding authors on reasonable request.

Results and Discussion

Severe hyperglycemia reduces GLP-1R mediated exendin uptake in murine islets

To analyze the effect of hyperglycemia on GLP-1R mediated exendin uptake, chemically-induced diabetic mice were transplanted with a submarginal islet mass and blood glucose levels were regulated with insulin implants (Fig.1A). Hyperglycemia had a substantial effect on exendin uptake, evidenced from ^{111}In -exendin SPECT scans (Fig.1B) and autoradiography images (inserts in Fig.2A-B). ^{111}In -exendin accumulation within islet grafts significantly decreased when islets were exposed to hyperglycemia (Control $1.19 \times 10^{-4} \pm 0.34 \times 10^{-4} \text{ Bq}/\mu\text{m}^2$ vs. Hyper $0.37 \times 10^{-4} \pm 0.22 \times 10^{-4} \text{ Bq}/\mu\text{m}^2$, $p < 0.001$) (Fig.1C). This was accompanied by a marked reduction in GLP-1R staining intensity compared to the control (Fig.2A,C), while the insulin staining intensity was maintained (Fig.2B,D). The observation that hyperglycemia reduced GLP-1R staining intensity implies that the reduced tracer uptake was caused by a reduction in GLP-1R expression, which is in line with previous *in vitro* reports (11,12).

Normalization of blood glucose levels restores GLP-1R mediated exendin uptake in murine islets

Since near-normalization of blood glucose levels improves beta-cell responsiveness to GLP-1 in patients with type 2 diabetes (19,20), we hypothesized that strict regulation of

blood glucose may reinstate GLP-1R expression. Normalization of blood glucose levels restored the observed decrease in tracer uptake (Control $1.19 \times 10^{-4} \pm 0.34 \times 10^{-4}$ Bq/ μm^2 vs. Restored $1.41 \times 10^{-4} \pm 0.27 \times 10^{-4}$ Bq/ μm^2 , $p = 0.40$) (Fig.1B-C), which was paralleled by normalization of GLP-1R staining intensity (Fig.2E).

Linear correlation between exendin uptake and beta-cell area is preserved after severe hyperglycemia

We have previously shown that exendin uptake linearly correlates with absolute BCM (8,9), indicating the potential of exendin as an imaging biomarker for BCM (7). To examine whether hyperglycemia affects this linear relationship, we correlated the uptake of exendin with the beta-cell area. Exendin uptake linearly correlated with the insulin-positive beta-cell area (Control, Pearson's $r = 0.89$, $p < 0.0001$) (Fig.1D). This linear correlation was maintained after a period of hyperglycemia (Hyper, Pearson's $r = 0.84$, $p < 0.0001$) (Fig.1D), though the slope of the correlation curve was significantly decreased compared to the control group (Hyper 0.36×10^{-4} vs. Control 1.29×10^{-4} , $p = 0.013$), reflecting the decrease in absolute uptake. Normalization of blood glucose levels completely reinstated the slope of the correlation curve (Restored 1.47×10^{-4} vs. Control 1.29×10^{-4} , $p = 0.51$) (Fig.1D).

Normalization of blood glucose levels restores exendin uptake in human islets

To assess whether these observations are representative for the human situation, we transplanted human islets into the anterior chamber of the eye of NOD-Scid mice. The advantage of this model is the ability to repetitively image an individual islet at a cellular resolution (21) using fluorescently labeled exendin. After engraftment, mice were imaged and distributed into two groups: one control group and one group receiving a single dose

of STZ to induce endogenous beta-cell destruction (22) (Fig.3B). One week after STZ treatment, a significant reduction in islet backscatter signal intensity was observed (Fig.3A,C), indicative for beta-cell exhaustion leading to degranulation (18). In this group, the exendin uptake progressively decreased to $34.45\pm0.07\%$ of the pre-treatment value (Fig.3D), which was accompanied by a reduction in islet volume (Fig.3E). Normalization of blood glucose levels (Fig.3B) resulted in cellular regranulation within a 3-week period and stabilization of the islet volume (Fig.3E), which is in agreement with previously reported data on human islet recovery in response to transient hyperglycemia (18). Tracer uptake was found to immediately improve after glycemic levels were restored. After 3 weeks of near-normalized blood glucose levels, tracer uptake was $76.81\pm0.07\%$ of the initial time-point (Fig.3D). This reduction in tracer uptake (23.19%) corresponded to the observed reduction in islet volume ($21.64 \pm 0.03\%$) (Fig.3E), which suggests that the reduction in tracer uptake may be attributed to hyperglycemia-induced loss in BCM. To test this hypothesis, sections of explanted eyes were immunostained for insulin (Fig.4A), revealing a significantly reduced insulin-positive area in the restored group compared to controls (Restored $26.30\pm0.55\%$ vs. Control $40.00\pm4.26\%$, $p < 0.05$) (Fig.4B). When we compared the tracer uptake in these islets at the last *in vivo* imaging time-point, a similar reduction in tracer uptake was observed (Restored $28.19\pm0.92\%$ vs. Control $36.81\pm3.63\%$, $p < 0.04$) (Fig.4C). These results indicate that a loss in BCM was responsible for the reduction in tracer uptake.

Taken together, our results highlight a critical role for hyperglycemia in GLP-1R regulation. Although hyperglycemia results in a substantial decrease in exendin uptake in murine and human islets, we have demonstrated that the uptake linearly correlates with BCM and that

normalization of blood glucose levels restores exendin uptake. The observed 3-fold reduction in tracer uptake in murine and human islets under hyperglycemic conditions may be an underestimation, as there are indications that hyperglycemia can increase capillary blood perfusion in islets (23). An important caveat of this study is that we used animal models with prolonged levels of hyperglycemia, whereas patients with diabetes experience fluctuating blood glucose levels, with 2h-postprandial blood glucose levels of at least 200 mg/dL (24–26). Therefore, the observed reduction in tracer uptake may not be as dramatic in patients as described here. Nevertheless, this manuscript emphasizes the potency and clinical relevance of nuclear imaging techniques to monitor receptor regulation non-invasively. Our results indicate that blood glucose levels should be near-normalized for at least three weeks prior to GLP-1R agonist treatment or radiolabeled exendin imaging for BCM quantification.

Author Contributions

MB, CC and WE contributed to the design, conduct, analysis, and interpretation of the data. MB and CC wrote and edited the manuscript. LCJ, CF, DB, and GS provided technical assistance in radiolabeling, tissue sectioning, immunostaining and imaging. MBr, SS and MG contributed to the experimental design, interpretation of the results, and conceptualization of the manuscript. SS and MG are the guarantors of this work and, as such, had full access to all the data in the study and take responsibility for the integrity of the data and the accuracy of the data analysis.

Acknowledgements

We thank the animal technicians for their assistance in animal care and data collection. This project is supported by BetaCure (FP7/2014–2018), Paul Langerhans Institute Dresden (PLID) of Helmholtz Zentrum München at the University Clinic Carl Gustav Carus of Technische Universität Dresden, the German Ministry for Education and Research (BMBF) to the German Centre for Diabetes Research (DZD) and the DFG - SFB/Transregio 127, and it has received funding from the Innovative Medicines Initiative 2 Joint Undertaking under grant agreement No 115797 (INNODIA) and No 945268 (INNODIA HARVEST). This Joint Undertaking receives support from the Union's Horizon 2020 research and innovation programme, "EFPIA", "JDRF" and "The Leona M. and Harry B. Helmsley Charitable Trust".

Competing interest

MG declares that he is an inventor and holder of the patent "Invention affecting GLP-1 and exendin" (Philipps-Universität Marburg, June 17, 2009). All other authors declare they have no conflicts of interest.

References

1. Song I, Muller C, Louw J, Bouwens L. Regulating the beta cell mass as a strategy for type-2 diabetes treatment. *Curr Drug Targets* [Internet]. 2015;16(5):516–24. Available from: <https://www.scopus.com/inward/record.uri?eid=2-s2.0-84929668026&partnerID=40&md5=36cd5ad3226cf21fee4903a52c7e648c>
2. Löhr M, Klöppel G. Residual insulin positivity and pancreatic atrophy in relation to duration of chronic Type 1 (insulin-dependent) diabetes mellitus and

- microangiopathy. *Diabetologia*. 1987;30:757–62.
3. Keenan H a, Sun JK, Levine J, Doria A, Aie LP. Residual Insulin Production and Pancreatic Beta-cell Turnover After 50 Year ... *Diabetes*. 2010;59(11):2846–53.
 4. Rahier J, Guiot Y, Goebbels RM, Sempoux C, Henquin JC. Pancreatic beta-cell mass in European subjects with type 2 diabetes. *Diabetes Obes Metab*. 2008;10 Suppl 4:32–42.
 5. Aguayo-Mazzucato C, Bonner-Weir S. Pancreatic β Cell Regeneration as a Possible Therapy for Diabetes. *Cell Metab* [Internet]. 2018;27(1):57–67. Available from: <https://doi.org/10.1016/j.cmet.2017.08.007>
 6. Krogvold L, Edwin B, Buanes T, Ludvigsson J, Korsgren O, Hy??ty H, et al. Pancreatic biopsy by minimal tail resection in live adult patients at the onset of type 1 diabetes: Experiences from the DiViD study. *Diabetologia*. 2014;57(4):841–3.
 7. Eriksson O, Laughlin M, Brom M, Nuutila P, Roden M, Hwa A, et al. In vivo imaging of beta cells with radiotracers: state of the art, prospects and recommendations for development and use. *Diabetologia* [Internet]. 2016;1–10. Available from: <http://dx.doi.org/10.1007/s00125-016-3959-7>
 8. Brom M, Woliner-van der Weg W, Joosten L, Frielink C, Bouckennooghe T, Rijken P, et al. Non-invasive quantification of the beta cell mass by SPECT with (111)In-labelled exendin. *Diabetologia* [Internet]. 2014 Feb 1 [cited 2014 Feb 7];57(5):950–9. Available from: <http://www.ncbi.nlm.nih.gov/pubmed/24488022>
 9. Brom M, Joosten L, Frielink C, Boerman O, Gotthardt M. 111In-exendin Uptake in the Pancreas Correlates With the β -Cell Mass and Not With the α -Cell Mass.

- Diabetes. 2015;64(4):1324–8.
10. Selvaraju RK, Velikyan I, Johansson L, Wu Z, Todorov I, Shively J, et al. In vivo imaging of the glucagonlike peptide 1 receptor in the pancreas with ⁶⁸Ga-labeled DO3A-exendin-4. *J Nucl Med* [Internet]. 2013;54(8):1458–63. Available from: <http://jnm.snmjournals.org/content/54/8/1458.long>
 11. Xu G, Kaneto H, Laybutt DR, Duvivier-Kali VF, Trivedi N, Suzuma K, et al. Downregulation of GLP-1 and GIP receptor expression by hyperglycemia: Possible contribution to impaired incretin effects in diabetes. *Diabetes*. 2007;56(June):1551–8.
 12. Rajan S, Dickson LM, Mathew E, Orr CMO, Ellenbroek JH, Philipson LH, et al. Chronic hyperglycemia downregulates GLP-1 receptor signaling in pancreatic β -cells via protein kinase A. *Mol Metab* [Internet]. 2015;4(4):265–76. Available from: <http://linkinghub.elsevier.com/retrieve/pii/S221287781500023X>
 13. Brom M, Oyen WJG, Joosten L, Gotthardt M, Boerman OC. ⁶⁸Ga-labelled exendin-3, a new agent for the detection of insulinomas with PET. *Eur J Nucl Med Mol Imaging* [Internet]. 2010;37(7):1345–55. Available from: <http://www.pubmedcentral.nih.gov/articlerender.fcgi?artid=2886138&tool=pmcentrez&rendertype=abstract>
 14. Ballerstadt R, Gowda A. Continuous Glucose Monitoring in Normal Mice and Mice with Prediabetes and Diabetes. *DIABETES Technol Ther*. 2006;8:402–12.
 15. Eter WA, Bos D, Frielink C, Boerman OC, Brom M, Gotthardt M. Graft revascularization is essential for non-invasive monitoring of transplanted islets with radiolabeled exendin. *Sci Rep* [Internet]. 2015;5(October):15521. Available

from:

<http://www.nature.com/articles/srep15521>
<http://www.ncbi.nlm.nih.gov/pubmed/26490110>

16. Cohrs CM, Chen C, Jahn SR, Stertmann J, Chmelova H, Weitz J, et al. Vessel network architecture of adult human islets promotes distinct cell-cell interactions in situ and is altered after transplantation. *Endocrinology*. 2017;158(5):1373–85.
17. Eter WA, Van der Kroon I, Andralojc K, Buitinga M, Willekens SMA, Frielink C, et al. Non-invasive in vivo determination of viable islet graft volume by ¹¹¹In-exendin-3. *Sci Rep* [Internet]. 2017;7(1):7232. Available from: <http://www.nature.com/articles/s41598-017-07815-3>
18. Chmelova H, Cohrs CM, Chouinard JA, Petzold C, Kuhn M, Chen C, et al. Distinct roles of Beta-Cell mass and function during type 1 diabetes onset and remission. *Diabetes*. 2015;64(6):2148–60.
19. Højberg P V., Zander M, Vilsbøll T, Knop FK, Krarup T, Vølund a., et al. Near normalisation of blood glucose improves the potentiating effect of GLP-1 on glucose-induced insulin secretion in patients with type 2 diabetes. *Diabetologia*. 2008;51(4):632–40.
20. Højberg P V., Vilsbøll T, Rabøl R, Knop FK, Bache M, Krarup T, et al. Four weeks of near-normalisation of blood glucose improves the insulin response to glucagon-like peptide-1 and glucose-dependent insulinitropic polypeptide in patients with type 2 diabetes. *Diabetologia*. 2009;52(2):199–207.
21. Speier S, Nyqvist D, Cabrera O, Yu J, Molano RD, Pileggi A, et al. Noninvasive in vivo imaging of pancreatic islet cell biology. *Nat Med* [Internet]. 2008;14(5):574–

8. Available from:

<http://www.pubmedcentral.nih.gov/articlerender.fcgi?artid=3538807&tool=pmcentrez&rendertype=abstract>

22. Yang H, Wright JR. Human β cells are exceedingly resistant to streptozotocin in vivo. *Endocrinology*. 2002;143(7):2491–5.
23. Menger MD, Vajkoczy P, Leiderer R, Jager S, Messmer K. Influence of experimental hyperglycemia on microvascular blood perfusion of pancreatic islet isografts. *J Clin Invest*. 1992;90(4):1361–9.
24. Of D, Mellitus D. Diagnosis and classification of diabetes mellitus. *Diabetes Care*. 2014;37(SUPPL.1):81–90.
25. Silversmith J, Deeb L, Klingensmith G, Grey M, Copeland K, Anderson B, et al. Care of Children and Adolescents With Type 1 Diabetes A statement of the American Diabetes Association. *Diabetes Care*. 2005;28(1):186–212.
26. Harris MI, Klein R, Welborn TA, Knuiman MW. Onset of NIDDM occurs at least 4-7 yr before clinical diagnosis. *Diabetes Care*. 1992;15(7):815–9.

Figure legends

Figure 1. GLP-1R mediated exendin uptake is significantly reduced in murine islets after sustained hyperglycemia, which is restored upon normalization of glycemic levels.

(A) Blood glucose (BG) levels of murine syngeneic islet transplants. After hyperglycemia was confirmed, mice received subcutaneous insulin implants to normalize blood glucose levels prior to islet transplantation. Two weeks after transplantation, mice were randomly assigned to one out of three experimental groups (Control, Hyper and Restored). The blood glucose levels of the control group were maintained within physiological range with insulin pellets (BG<200 mg/dL). Insulin pellets were removed from mice assigned to the Hyper or Restored group to induce severe hyperglycemia (BG>350 mg/dL). After four weeks of hyperglycemia, mice assigned to the Restored group received insulin pellets again for a period of three weeks. **(B)** ^{111}In -labeled exendin-3 SPECT/CT scans of Control, Hyper, and Restored mice. **(C)** GLP-1R mediated exendin-3 uptake in islets in the Control, Hyper and Restored groups. Data are presented as mean \pm SEM. *** = p-value < 0.001 and ****= p-value < 0.0001, evaluated by ANOVA with Tuckey post-hoc test with n=6 per group, scale bars = 100 μm . **(D)** Correlation between exendin-3 uptake and beta-cell area in the Control, Hyper and Restored groups. The slope of the correlation curve was significantly decreased in the hyper group compared to the control group (p=0.013). Normalization of blood glucose levels completely restored the slope of the correlation curve (p=0.51).

Figure 2. Anti-insulin and GLP-1R staining of islet grafts in Control, Hyper and Restored mice.

(A-F) immunohistochemistry images of islet grafts stained for GLP-1R of Control (A), Hyper (C) and Restored (E) mice and for insulin of Control (B), Hyper (D) and Restored (F) mice. Inserts in (A, C, E) depict autoradiography images of grafts with comparable insulin areas. Scale bars = 100 μ m.

Figure 3. Exendin uptake in human islets depends on the glycemic status of the recipient.

(A) Maximum intensity projections (MIP) of the same human islets in the Control and Restored group with islet backscatter (grey) and alexa647 labeled exendin-3 (magenta) at indicated time points. (B) Blood glucose profile of the Control and Restored group throughout the experiment. (C-E) Quantification of (C) backscatter signal in transplanted human islets, (D) exendin3+ islet volume and (E) islet volume relative to the initial imaging time point. In B-E first dotted line indicates STZ injection and second dotted line indicates insulin pellet implantation; red background indicates the period of hyperglycemia in the Restored group. n=3 mice (Control), 4 mice (Restored) with 16 and 22 individual islets respectively. Data are presented as mean \pm SEM, * = p-value <0.05 evaluated by mixed model analysis; scale bars = 50 μ m

Figure 4. Insulin area correlates with exendin uptake in human islets

(A) Images of explanted islets after termination of the experiment stained for insulin (green, left panel) as well as glucagon (magenta) and DAPI (blue) (merged image, right panel).

(B) Quantification of Ins⁺ islet area in sections and **(C)** % exendin3⁺ islet volume at the last in vivo imaging time point. Data are presented as mean±SEM, * = p-value < 0.05 evaluated by Mann-Whitney rank sum test with n=3 mice (Control) and 4 mice (Restored); scale bars = 50 μm.

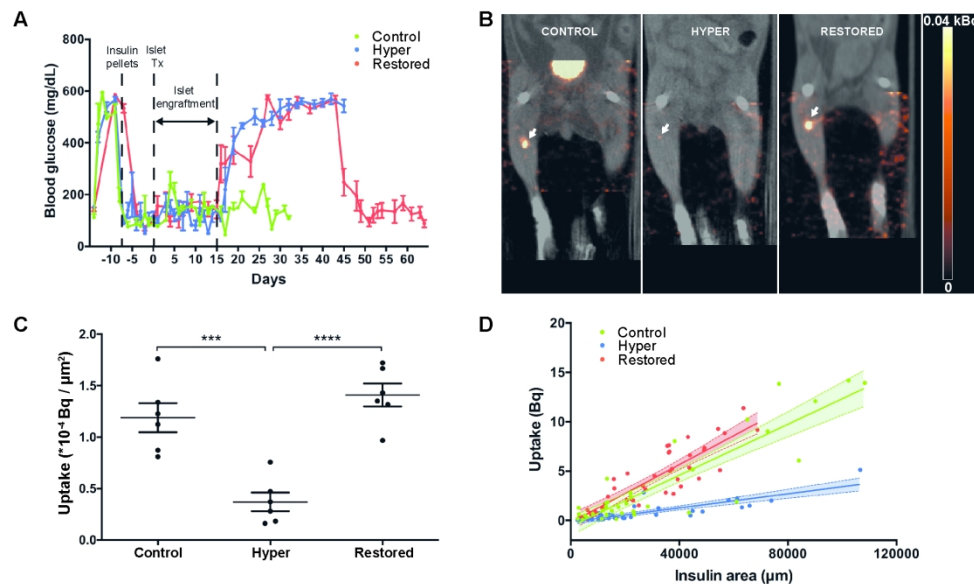


Figure 1. GLP-1R mediated exendin uptake is significantly reduced in murine islets after sustained hyperglycemia, which is restored upon normalization of glycemic levels. (A) Blood glucose (BG) levels of murine syngeneic islet transplants. After hyperglycemia was confirmed, mice received subcutaneous insulin implants to normalize blood glucose levels prior to islet transplantation. Two weeks after transplantation, mice were randomly assigned to one out of three experimental groups (Control, Hyper and Restored). The blood glucose levels of the control group were maintained within physiological range with insulin pellets (BG < 200 mg/dL). Insulin pellets were removed from mice assigned to the Hyper or Restored group to induce severe hyperglycemia (BG > 350 mg/dL). After four weeks of hyperglycemia, mice assigned to the Restored group received insulin pellets again for a period of three weeks. (B) ^{111}In -labeled exendin-3 SPECT/CT scans of Control, Hyper, and Restored mice. (C) GLP-1R mediated exendin-3 uptake in islets in the Control, Hyper and Restored groups. Data are presented as mean \pm SEM. *** = p-value < 0.001 and **** = p-value < 0.0001, evaluated by ANOVA with Tuckey post-hoc test with n=6 per group, scale bars = 100 μm . (D) Correlation between exendin-3 uptake and beta-cell area in the Control, Hyper and Restored groups. The slope of the correlation curve was significantly decreased in the hyper group compared to the control group (p=0.013). Normalization of blood glucose levels completely restored the slope of the correlation curve (p=0.51).

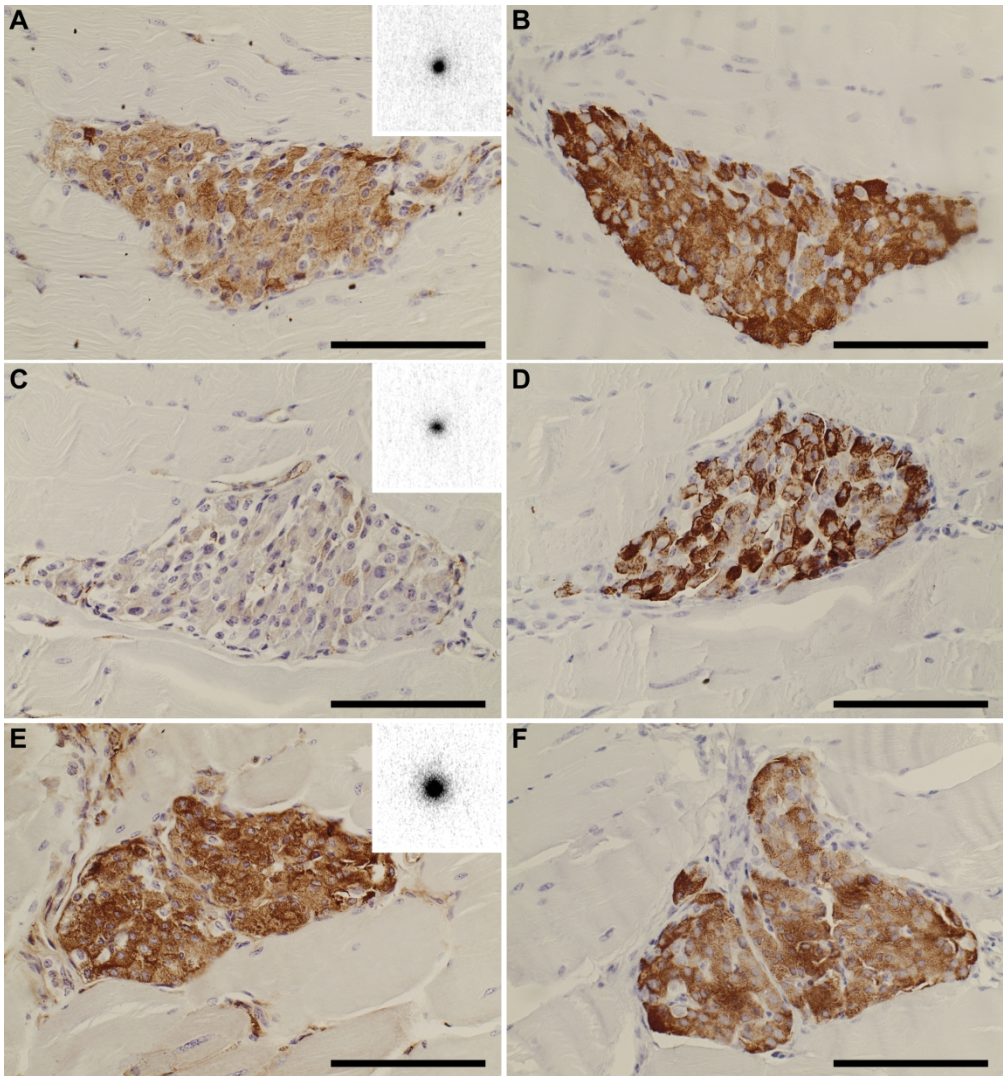


Figure 2. Anti-insulin and GLP-1R staining of islet grafts in Control, Hyper and Restored mice. (A-F) immunohistochemistry images of islet grafts stained for GLP-1R of Control (A), Hyper (c) and Restored (E) mice and for insulin of Control (B), Hyper (D) and Restored (F) mice. Inserts in (A, C, E) depict autoradiography images of grafts with comparable insulin areas. Scale bars = 100 μ m.

874x937mm (72 x 72 DPI)

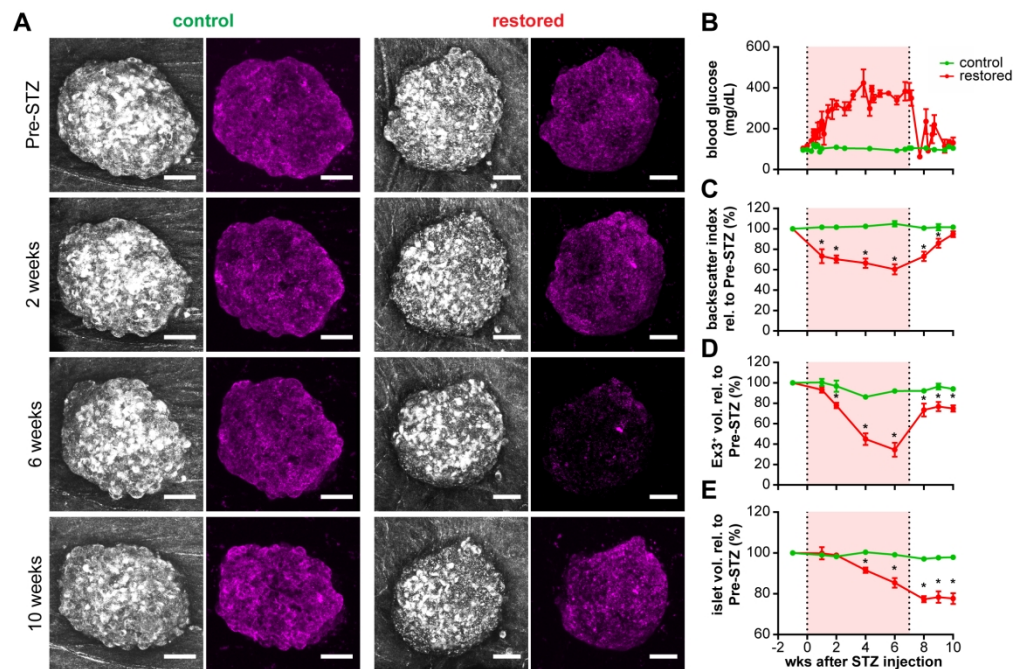


Figure 3. Exendin uptake in human islets depends on the glycemic status of the recipient. (A) Maximum intensity projections (MIP) of the same human islets in the Control and Restored group with islet backscatter (grey) and alexa647 labeled exendin-3 (magenta) at indicated time points. (B) Blood glucose profile of the Control and Restored group throughout the experiment. (C-E) Quantification of (C) backscatter signal in transplanted human islets, (D) exendin3+ islet volume and (E) islet volume relative to the initial imaging time point. In B-E first dotted line indicates STZ injection and second dotted line indicates insulin pellet implantation; red background indicates the period of hyperglycemia in the Restored group. n=3 mice (Control), 4 mice (Restored) with 16 and 22 individual islets respectively. Data are presented as mean±SEM, * = p-value <0.05 evaluated by mixed model analysis; scale bars = 50 μ m

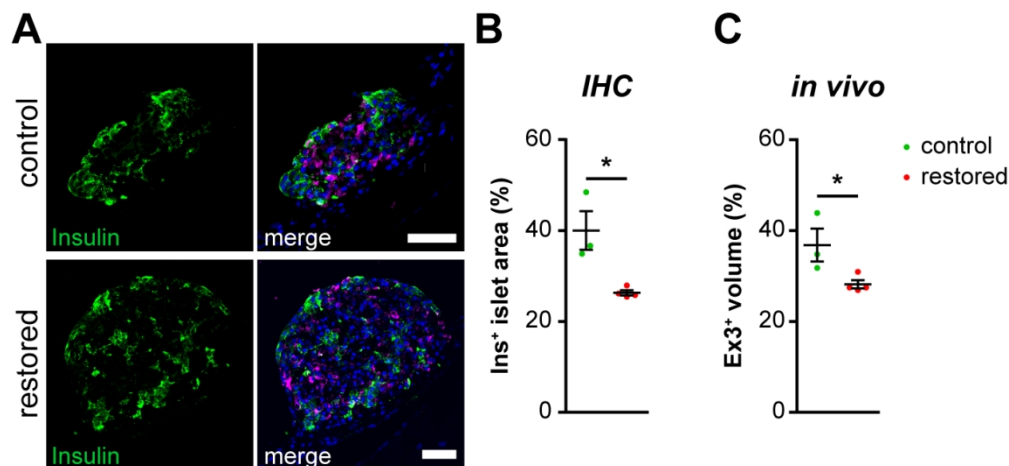


Figure 4. Insulin area correlates with exendin uptake in human islets
(A) Images of explanted islets after termination of the experiment stained for insulin (green, left panel) as well as glucagon (magenta) and DAPI (blue) (merged image, right panel). (B) Quantification of Ins+ islet area in sections and (C) % exendin3+ islet volume at the last in vivo imaging time point. Data are presented as mean±SEM, * = p-value < 0.05 evaluated by Mann-Whitney rank sum test with n=3 mice (Control) and 4 mice (Restored); scale bars = 50 μ m.

Checklist for Reporting Human Islet Preparations Used in Research

Adapted from Hart NJ, Powers AC (2018) Progress, challenges, and suggestions for using human islets to understand islet biology and human diabetes. Diabetologia <https://doi.org/10.1007/s00125-018-4772-2>.

Manuscript DOI: https://doi.org/10.2337/DB20-0616	
Title: Non-invasive monitoring of glycemia-induced regulation of GLP-1R expression in murine and human islets of Langerhans	
Author list: M.Buitinga, C.M.Cohrs, W.A.Eter, L.Claessens-Joosten, C.Frieling, D.Bos, G. Sandker, M.Brom, S.Speier, M.Gotthardt	
Corresponding author: Mijke Buitinga	Email address: mijkebuitinga@hotmail.com

Islet preparation	1	2	3	4	5	6	7	8 ^a
MANDATORY INFORMATION								
Unique identifier	Lot HP-17075-01							
Donor age (years)	37							
Donor sex (M/F)	F							
Donor BMI (kg/m ²)	19.57							

Donor HbA _{1c} or other measure of blood glucose control	4.6%							
Origin/source of islets ^b	Prodo Laboratories							
Islet isolation centre	Prodo Laboratories							
Donor history of diabetes? Yes/No	No							
If Yes, complete the next two lines if this information is available								
Diabetes duration (years)								
Glucose-lowering therapy at time of death ^c								

RECOMMENDED INFORMATION								
Donor cause of death	anoxic event							
Warm ischaemia time (h)								
Cold ischaemia time (h)								

Estimated purity (%)	90							
Estimated viability (%)	90							
Total culture time (h) ^d	o.n. after receiving							
Glucose-stimulated insulin secretion or other functional measurement ^e								
Handpicked to purity? Yes/No	Yes							
Additional notes								

^aIf you have used more than eight islet preparations, please complete additional forms as necessary

^bFor example, IIDP, ECIT, Alberta IsletCore

^cPlease specify the therapy/therapies

^dTime of islet culture at the isolation centre, during shipment and at the receiving laboratory

^ePlease specify the test and the results